



Published in final edited form as:

Transl Res. 2021 September ; 235: 32–47. doi:10.1016/j.trsl.2021.03.005.

## Identification of novel therapeutic targets for contrast induced acute kidney injury (CI-AKI): alpha blockers as a therapeutic strategy for CI-AKI

SREENIVASULU KILARI, AMIT SHARMA, CHENGLI ZHAO, AVISHEK SINGH, CHUANQI CAI, MICHAEL SIMEON, ANDRE J. VAN WIJNEN, SANJAY MISRA

Vascular and Interventional Radiology Translational Laboratory, Department of Radiology, Mayo Clinic, Rochester, Minnesota; Depart-Department of Vascular Surgery, The Second Xiangya Hospital, Central South University, Changsha, Hunan, China; Department of Vascular Surgery, Union Hospital, Tongji Medical College, Huazhong University of Science and Technology, Wuhan, China; Department of Biochemistry and Molecular Biology, Mayo Clinic, Rochester, Minnesota; Orthopedic Surgery, Mayo Clinic, Rochester, Minnesota; Department of Pulmonary and Critical Care Medicine Mayo Clinic, Rochester, Minnesota.

### Abstract

Iodinated contrast is used for imaging and invasive procedures and it can cause contrast induced acute kidney injury (CI-AKI), which is the third leading hospital-acquired health problem. The purpose of the present study was to determine the effect of  $\alpha$ -adrenergic receptor-1b (*Adra1b*) inhibition by using terazosin on change in kidney function, gene, and protein expression in C57BL/6J male mice, 6–8 weeks with chronic kidney disease (CKD). CKD was induced by surgical nephrectomy. Twenty eight days later, 100- $\mu$ L of iodinated contrast (CI group) or saline (S group) was given via the carotid artery. Whole-transcriptome RNA-sequencing (RNA-Seq) analysis of the kidneys was performed at day 2. Mice received either 50- $\mu$ L of saline ip or terazosin (2 mg/kg) in 50- $\mu$ L of saline ip 1 hour before contrast administration which was continued every 12 hours until the animals were euthanized 2 and 7 days later. The kidneys were removed for gene expression, immunohistochemical analysis, and blood serum analyzed for kidney function. Differential gene expression analysis identified 21 upregulated and 436 downregulated genes (fold change  $>2$ ;  $P < 0.05$ ) that were common to all sample ( $n = 3$  for both contrast and saline). We identified *Adra1b* using bioinformatic analysis. Mice treated with terazosin had a significant decrease in serum creatinine, urinary Kim-1 levels, HIF-1 $\alpha$ , apoptosis, and downstream *Adrab1* genes including *Ece1*, *Edn1*, pMAPK14 with increased cell proliferation. Contrast exposure upregulated *Adra1b* gene expression in HK-2 cells. Inhibition of *Adra1b* with

Reprint requests: Sanjay Misra, Mayo Clinic, Department of Radiology, Professor of Radiology, 200 First Street SW, Rochester, MN 55905. misra.sanjay@mayo.edu.

Author contributions are as follows: S.K. and S.M. designed the study, SK performed significant parts of the experiments and contributed to animal surgery, SK, AW and SM contributed to the gene enrichment analysis, S.K., A.S., and S.M. contributed to data organization and discussion, S.K. and S.M. wrote the manuscript.

Conflicts of interest: The authors declare that they have no competing interests.

The authors have read the manuscript and agree with it. All authors have read the journal's policy on conflicts of interest and authorship agreement.

### SUPPLEMENTARY MATERIALS

Supplementary material associated with this article can be found in the online version at doi:10.1016/j.trsl.2021.03.005.

terazosin abrogated *Ece1*, *Edn1*, and contrast-induced *Fsp-1*, *Mmp-2*, *Mmp-9* expression, and caspase-3/7 activity in HK-2 cells.

---

## INTRODUCTION

Iodinated radiocontrast agents are used widely when performing minimally invasive catheter-based procedures and diagnostic imaging. Their use can cause acute kidney injury, referred to as contrast induced acute kidney injury (CI-AKI). CI-AKI is the third leading hospital-acquired health problem.<sup>1</sup> In patients with normal kidney function, CI-AKI occurs in 5% of the patients, but its prevalence is higher in patients with chronic kidney diseases (CKD), diabetes, cardiovascular diseases, infection and inflammation.<sup>1-4</sup> There is controversy on whether CI-AKI occurs in patients administered intravenous contrast.<sup>5-7</sup> McDonald et al. concluded that CI-AKI risk depends on pre-existing clinical conditions rather than the intravenous route of contrast administration.<sup>8</sup> It is well established that intra-arterial contrast administration is associated with CI-AKI.<sup>2,9,10</sup> Multiple therapies have been tried to reduce CI-AKI including n-acetyl cysteine and alprostadil but currently there are few therapies that can prevent CI-AKI.<sup>11,12</sup> Understanding the mechanisms responsible for CI-AKI could help to improve outcomes in patients at risk for it.

The molecular mechanisms involved in the pathogenesis of CI-AKI are not well understood. It is postulated that hypoxia due to vasoconstriction, oxidative stress, inflammation of tubular cells and nephrons caused by exposure to the highly-concentrated contrast medium during the filtration process are involved in the pathogenesis.<sup>2,13</sup> In order to understand the mechanisms of CI-AKI, experimental animal models were created in mice with established chronic kidney disease.<sup>14,15</sup> Using this model, we demonstrated that there is upregulation of TGF- $\beta$ 1 (TGF $\beta$ 1)/SMAD3 signaling in kidneys two days after intra-arterial or intravenous contrast administration.<sup>14,15</sup> Moreover, blockade of TGF- $\beta$ /SMAD3 signaling using a TGF- $\beta$ R1 (TGF $\beta$ R1) inhibitor in epithelial cells isolated from human kidney proximal tubules (HK-2 cells) resulted in a decrease in contrast-induced profibrotic genes downstream to TGF- $\beta$ 1 signaling.<sup>15</sup>

In the present study, we performed whole-transcriptome RNA-Seq analysis of kidneys removed from CKD mice 2 days after intra-arterial contrast administration. Gene enrichment and functional analysis of differentially regulated genes was performed.  $\alpha$ -adrenergic receptor-1b (ADRA1B) was found to be upregulated in contrast administered kidneys and in HK-2 cells after contrast exposure. ADRA1B is a heteromeric G-protein and belongs to the  $\alpha$ -adrenergic receptor-1 family. ADRA1B mediates its action by binding epinephrine and norepinephrine.<sup>16</sup> Alpha 1 receptor is involved in vasoconstriction by smooth muscle cells. Terazosin is a FDA approved  $\alpha$ 1-blocker and competes with epinephrine and norepinephrine binding to ADRA1B.<sup>17</sup> It is used to treat benign prostatic hyperplasia, hypertension and ureteral calculi.<sup>18</sup> We evaluated the effect of ADRA1B inhibition using terazosin in preventing CI-AKI in CKD mouse and in cell culture using HK-2 cells.

## MATERIALS AND METHODS

All antibodies and their dilutions used in the study are listed in Supplementary Table 1. HK-2 cells were purchased from ATCC (cat# CRL-2190, Manassas, VA). Cell culture media was obtained from Thermo Fisher Scientific (Waltham, MA) unless specified otherwise. Radiocontrast Visipaque (iodoxinol) was purchased from GE Healthcare (Chicago, IL). Terazosin was purchased from Cayman Chemical (cat# 63074-08-8, Ann Arbor, MI). All other chemicals were purchased from Sigma Aldrich (St. Louis, MO) unless specified otherwise.

### Animal experiments.

Approval was obtained from the Mayo Clinic Institutional Animal Care and Use Committee prior to performing animal experiments. C57BL/6J male mice, 6 to 8 weeks old, were obtained from Jackson Labs (Bar Harbor, ME) and maintained at standard conditions: 22°C temperature, 41% relative humidity, and 12-hour light-dark cycles. Animals were allowed access to water and food *ad libitum*.

### Creation of a chronic kidney disease model.

Chronic kidney disease (CKD) was created as described previously.<sup>19,20</sup> Briefly, the left kidney was removed and the upper pole of the right kidney renal artery was ligated.

### Contrast administration.

Twenty-one days later, we assessed the BUN and creatinine of the animals and selected those that had an average creatinine greater than 0.3 mg/dL.<sup>14</sup> Twenty eight days after nephrectomy, contrast was administered via the right or left carotid artery using a polyethylene capillary catheter (Cat#427410; Intragenic Becton, Dickenson and Company; Franklin Lakes, NJ). 100- $\mu$ L of iodinated contrast (CI group) or saline (S group) was injected at 10- $\mu$ L/min flow rate using a syringe pump. The carotid artery was ligated using 10-0 suture and the incision was closed with 6-0 suture. Mice received IP injection of either 50- $\mu$ L of saline or terazosin (2 mg/kg) in 50- $\mu$ L of saline 1 hour before contrast administration (CI+T) and this was repeated every 12 hours until the animals were euthanized. The study design is shown in Supplementary Fig 1.

### Sample collection.

At day 2 or 7 after contrast administration, mice were euthanized, and the kidney was excised and divided into two parts using a sagittal cut. One part was stored in 4% buffered formalin for immunohistochemical analysis. The other part was further dissected to separate the medulla and the cortex and then stored in RNAlater (Qiagen, Germantown, MD) for RNA isolation and subsequent gene expression studies. Blood and urine were collected before nephrectomy (BL), 28 days after nephrectomy before contrast or saline administration (D0), day 2 (D2) and day 7 (D7) after contrast or saline administration.

### **Serum creatinine, blood urea and urinary kidney injury molecule-1 analysis.**

Serum creatinine and blood urea nitrogen were determined using a serum creatinine colorimetric assay kit (Cat# 700460, Cayman Chemical, Ann Arbor MI) and the QuantiChrome urea assay kit (Cat# DIUR-100, BioAssay Systems, Hayward, CA) respectively.<sup>21,22</sup> Urinary KIM-1 levels were assessed using the KIM-1 ELISA kit (Cat#MKM100, R&D Systems, Minneapolis, MN) following manufacturer's instructions.

### **RNA sequencing and bioinformatics analysis.**

Total RNA was isolated using miRNeasy kit (cat# 217604, Qiagen), and whole transcriptomic mRNA-Seq was performed at the Mayo Clinic Medical Genome Facility.<sup>23</sup> RNA libraries were prepared using the TruSeq RNA sample kit V2 (Illumina, San Diego, CA) following the manufacturer's protocol. mRNA libraries were loaded into flow cells (TruSeq v3 paired-end flow cells; Illumina) at concentrations designed to generate 100 million total reads/sample following Illumina's standard protocol using the Illumina cBot and TruSeq Paired end cluster kit version 3. The flow cells were then sequenced on HiSeq 2000/2500 using the TruSeq SBS sequencing kit version 3 (Illumina) and the data was collected using HiSeq data collection version 2.0.12.0 software. Base-calling was performed using Illumina's RTA version 1.17.21.3. Data analysis was further performed using the MAPR Seq v.1.2.1 system, the Bioinformatics Core standard tool, Top Hat 2.0.6 and Feature Counts software.<sup>21,24</sup> Gene expression was standardized to 1 million reads and normalized for gene length (reads per kilobase pair per million mapped reads, RPKM). The mRNAs with a fold change of >2 and <0.5 were considered up regulated and down regulated, respectively, in kidneys of mice administered with either CI or S. A student t-test was performed and the difference in the fold change was considered statistically significant if  $P < 0.05$ . The mRNA list was then uploaded to Gene-E (<https://software.broadinstitute.org/GENE-E>) to create a heat map. PANTHER (<http://pantherdb.org/>) and DAVID 6.7 databases (<https://david-d.ncifcrf.gov/>) were used to determine the mRNA functional significance, cellular localization, biological process, and pathway analysis. Functional protein network analysis using String database<sup>25</sup> was used to determine the molecular interactions.

### **Cell culture.**

Human kidney proximal tubules (HK-2 cells) cells were cultured and maintained in DMEM/F12 medium.<sup>15</sup> Cells were treated with contrast medium diluted in DMEM/F12 medium at a concentration of 200 mg of Iodine/mL (mgI/mL) at different time points as indicated in the presence or absence of 1 $\mu$ M terazosin. For controls, cells were treated with PBS equivalent of the volume of contrast medium that was added to DMEM/F12. At the end of the treatment, cells were washed in ice-cold PBS and lysed in RIPA buffer with protease and phosphatase inhibitors for Western blot. For gene expression studies, cells were lysed in QIAzol and RNA was isolated using the miRNeasy kit (Qiagen, Germantown, MD).

### **cDNA synthesis and qRT-PCR for gene expression.**

cDNA was prepared from 100-ng of RNA using the IScript cDNA synthesis kit (Bio-Rad, Hercules, CA). Gene expression was assessed by performing qRT-PCR in a CFX-96 real-time PCR system using the iTaq-SYBR green master mix (Bio-Rad). The fold change in

gene expression was calculated following the  $2^{-\text{ct}}$  method after normalizing with 18S RNA gene expression with respective controls. The primers used to assess gene expression are listed in Supplementary Table 2.

### **Immunohistochemistry and TUNEL staining.**

Paraffin-embedded tissue sections were stained for ADRA1B, HIF-1 $\alpha$ , Ki-67, and pMAPK14 (pP38A) after heat-induced antigen retrieval as described previously.<sup>14,15</sup> TUNEL staining was performed using a TdT in-situ apoptosis detection kit (Cat# 4810–30K, R&D Systems, Minneapolis, MN) following the manufacturer's protocol and slides were counter-stained for Hematoxylin. Images of the entire tissue section were acquired at 10X magnification using a Zeiss Axio Imager-M2 equipped with a Zeiss Axiocam 503 Color camera (Zeiss, Oberkochen, Germany) and a motorized stage. The color intensity of immune positive staining was quantified using Zen Pro 2.0 software (Zeiss) as described previously.<sup>14</sup>

### **Co-immune staining for ADRA1b and pMAPK14.**

After de-paraffinization and heat induced antigen retrieval, tissue sections were blocked with 5% normal donkey serum for one hour at room temperature and overnight for rabbit anti pMAPK antibody (Cat# LC-C117441, LSBio, Seattle, WA). After washing, the sections were incubated with Alexa 594 conjugated donkey Anti Rabbit IgG for 1h at room temperature. The sections were washed and then blocked with 5% normal rabbit serum followed by 10- $\mu\text{g/ml}$  Donkey anti-rabbit IgG FAB fragment. After washing, the slides were then incubated with rabbit anti-ADRA1B antibody for 2h at room temperature followed by Alexa 488 conjugated donkey Anti Rabbit IgG for 1h at room temperature and counter stained with DAPI. The staining protocol was repeated without the primary antibody to serve as negative controls.

### **Caspase 3/7 assay.**

HK-2 cells ( $1 \times 10^4$ /well) were seeded in a 96-well plate. After overnight serum starvation, cells were incubated in serum-free medium with PBS (S), medium with contrast (CI) or contrast plus 1 $\mu\text{M}$  terazosin (CI+T) for 24 hours. Caspase3/7 assay was performed using the Caspase-Glo 3/7 assay system (Cat# G8090, Promega, Madison, WI) following the manufacturer's protocol.

### **Statistical analysis.**

All data were expressed as mean  $\pm$  standard error mean (SEM). Statistical differences were tested by either a one-way or two-way analysis of variance (ANOVA) followed by a post hoc Student *t*-test with Bonferroni's correction using Graph pad prism 8.0 (Graph Pad Software Inc, La Jolla, CA). The level of significance was set at \*  $P < 0.05$ .

## RESULTS

### Identification and classification of differentially expressed genes.

We first performed whole transcriptomic analysis using RNA sequencing performed on kidneys removed from mice with CKD two days after contrast (CI) or saline (S) administration. A heat map was created of all genes that were common to each sample with a greater than 2 fold increase or less than 0.5 fold decrease at a  $P < 0.05$  (Fig 1, A). We identified 21 genes that were upregulated [ $FC > 2$  (Fig 1, B)] and 436 genes that were down regulated ( $FC < 0.5$ ) (Fig 1, A and Supplementary Table 3).

Next, we determined the different functions of the up regulated genes based on molecular function, cellular component, protein class and pathway (Supplementary Fig 2). Molecular function analysis demonstrated that the majority of the genes are involved in catalytic activity (25%) followed by binding activity (15%) (Supplementary Fig 2, A). Analysis based on the cellular function demonstrated that most of the genes are related to membrane (37%) and extracellular proteins (27%), including proteins involved in matrix deposition (Supplementary Fig 2, B). Protein functional classification (Supplementary Fig 2, C) and pathway analysis (Supplementary Fig 2, D) revealed a significant presence of genes involved in cell-cell junctions, membrane trafficking and transcription factors related to G-protein signaling, alpha adrenergic receptor signaling and the plasminogen activating cascade.

Functional classification and molecular function analysis for down regulated genes revealed that majority of the genes were related to transcription factors, transporters, the cytoskeleton and oxidoreductase enzymes, binding, catalytic activity and the cell cycle (Supplementary Fig 3, A–C). We next determined the function of the down regulated genes and found that the genes related to integrin signaling, inflammation and angiogenesis were significantly down regulated ( $< 0.5$  fold, Supplementary Fig 3, D).

We performed analysis to identify upstream regulator molecules involved in the differentially regulated genes using Ingenuity Pathway Analysis (IPA). This revealed that TGF- $\beta 1$  is upstream to 7 of the 21 (33%) up regulated genes (Fig 2, A and B). Results from the functional protein-association network analysis (String database at <https://string-db.org/>) of upregulated genes showed that there were two different clusters of interactors with TGF- $\beta 1$  (Fig 2, C). This included profibrotic genes such as *Col-1a1*, *Des*, and *Lox1* that interact with TGF- $\beta 1$  via SMAD3 and *Ecml*. The second cluster involved *Fgg* and *Adralb*. A similar analysis was performed for down regulated genes but no upstream targets were identified that were statistically significant.

To further investigate these findings, Network-disease and functional analysis was performed using the IPA tool for down regulated genes. As shown in supplementary Fig 4, the top three functional clusters were related to organismal injury and abnormalities (Score-58, focus molecules 32), molecular transport (Score-50, focus molecules 29), DNA replication, recombination and repair, and gene expression (Score-47, focus molecules 28).

### Validation of RNA-Seq analysis.

qRT-PCR analysis was performed to validate the RNA-Seq transcriptomic analysis. We found that *Col-1a1* (4.6 fold;  $P=0.0014$ ), *Adra1b* (3.1 fold;  $P=0.00028$ ), *Lox1l* (3.03 fold;  $P=0.03$ ), *TGF- $\beta$ 1* (2.2 fold;  $P=0.0017$ ) and *Marcks* (1.9 fold;  $P=0.0017$ ) were significantly higher in CI kidneys compared to S group in murine kidneys at day 2 after contrast (CI) administration compared to saline (S) controls (Fig 2, D).

### Terazosin treatment shows a decrease in serum creatinine and urinary KIM-1 levels in contrast injected animals compared to controls.

We next investigated the effect of terazosin on CI-AKI after contrast administration (CI + T) compared to contrast (CI) or saline (S). Our results demonstrated that there was a significant increase in serum creatinine at 2 days after contrast administration compared to S group (CI:  $0.50 \pm 0.02$ , S:  $0.43 \pm 0.01$  mg/dL, average increase: 17.5%,  $P=0.015$ , Fig 3, A). Terazosin treatment significantly decreased the serum creatinine at day 2 (CI + T:  $0.44 \pm 0.01$ , CI:  $0.50 \pm 0.023$ , average decrease 11.3%,  $P=0.027$ , Fig 3, A). There was no significant change in blood urea nitrogen<sup>22</sup> in the CI + T group compared to CI group (Fig 3, B). We assessed the extent of kidney damage following contrast administration using kidney injury molecule-1 (KIM-1). There was no difference between the KIM-1 levels at baseline or day 0 between the groups. At day 2, the average urinary KIM-1 level was significantly higher in the CI group animals compared to S group (CI:  $2.44 \pm 0.28$  ng/mg creatinine, S:  $0.81 \pm 0.14$  ng/mg creatinine, average increase: 303.3%,  $P<0.0001$ , Fig 3, C) and day 7 (CI:  $2.24 \pm 0.12$  ng/mg creatinine, S:  $1.1 \pm 0.1$  ng/mg creatinine, average increase: 204.5%,  $P<0.0001$ , Fig 3, C). At day 2, there was a significant decrease in the urinary KIM-1 levels in the CI + T group compared to the CI group (CI + T:  $1.80 \pm 0.095$  ng/mg creatinine, CI:  $2.44 \pm 0.28$  ng/mg creatinine, average decrease: 26.45%,  $P=0.0072$ ,) and day 7, it remained significantly lower (CI + T:  $1.61 \pm 0.1$  ng/mg creatinine, CI:  $2.24 \pm 0.12$  ng/mg creatinine, average decrease: 28.2%,  $P=0.0086$ , Fig 3, C). However, urinary KIM-1 levels were significantly higher in the CI + T group compared to the S group at day 2 (CI + T:  $1.80 \pm 0.095$  ng/mg creatinine, S:  $0.805 \pm 0.14$  ng/mg creatinine; average increase: 223%,  $P<0.0001$ ) and at day 7 (CI + T:  $1.61 \pm 0.1$  ng/mg creatinine, S:  $1.1 \pm 0.1$  ng/mg creatinine; average increase: 146.8%,  $P=0.0086$ , Fig 3, C).

### Terazosin treatment attenuates contrast-induced *Adra1b* gene expression.

qRT-PCR analysis demonstrated that there was a significant increase in *Adra1b* expression at day 2 in the cortex of the CI group compared to the S group (CI:  $5.22 \pm 1.25$ , S:  $1.02 \pm 0.11$ , average increase: 510.7%,  $P<0.0001$ , Fig 4, A) and in medulla at day 2 (CI:  $2.34 \pm 0.15$ , S:  $1.02 \pm 0.1$ , average increase: 229%,  $P<0.03$ , Fig 4, B) and at day 7 (CI:  $2.71 \pm 0.51$ , S:  $1.02 \pm 0.07$ , average increase: 265%,  $P<0.0076$ , Fig 4, B). Terazosin treatment (CI + T) had a significant reduction of *Adra1b* expression at day 2 in the cortex (CI+T:  $1.53 \pm 0.28$ , CI:  $5.22 \pm 1.25$ , average decrease: 70.7%,  $P<0.0001$ , Fig 4, A) and medulla (CI+T:  $0.51 \pm 0.2$ , CI:  $2.34 \pm 1.5$ , average decrease: 78.2%,  $P<0.0040$ , Fig 4, B). Immunohistochemical analysis showed that ADRA1B staining was significantly increased in the cortex at day 2 (CI:  $15.29 \pm 0.97$ , S:  $6.28 \pm 1.82$ , average increase: 243.5%,  $P=0.018$ , Fig 4, C and D) and at day 7 (CI:  $11.61 \pm 1.41$ , S:  $3.44 \pm 0.19$ , average increase: 341.5%,  $P=0.039$ , Fig 4, E and

F). Terazosin treatment decreased ADRA1B staining in the cortex at day 2 compared to CI group (CI+T:  $8.88 \pm 1.77$ , CI:  $15.29 \pm 0.97$ , average decrease: 42%,  $P < 0.028$ , Fig 4, C and D). However, there was a significant increase in ADRA1B staining in CI+T group compared to S group cortex at 7 days after contrast administration (Fig 4, C and D).

ADRA1B staining was increased in the medulla at day2 (CI:  $9.84 \pm 1.89$ , S:  $3.77 \pm 0.76$ , average increase: 260.7%,  $P = 0.0005$ , Fig 4, E and F) and at day 7 (CI:  $7.83 \pm 1.52$ , S:  $3.28 \pm 0.46$ , average increase: 238.4%,  $P = 0.0064$ , Fig 4, E and F) in CI group compared to S group. Terazosin treatment showed a significant decrease in ADRA1B staining in the medulla at day 2 (CI+T:  $2.54 \pm 0.52$ , CI:  $9.84 \pm 1.89$ , average decrease: 74.16,  $P < 0.0001$ , Fig 4, C and D).

### **Terazosin treatment attenuates MAPK14 staining in murine kidneys with contrast administration.**

We next assessed MAPK14 phosphorylation a downstream signaling molecule to ADRA1B signaling by immunostaining. There was a significant increase in phospho-MAPK14 (pMAPK14) staining in the cortex after contrast administration compared to controls at day 2 (CI:  $22.04 \pm 4.80$ , S:  $1.81 \pm 0.89$ , average increase: 1259.7%;  $P < 0.0001$ , Fig 4, G and H) and day 7 (CI:  $7.87 \pm 0.26$ , S:  $0.37 \pm 0.10$ , average increase: 2131.4%;  $P = 0.012$ ). Terazosin treatment significantly decreased pMAPK14 staining in the cortex at day 2 (CI + T:  $3.28 \pm 0.99$ , CI:  $22.035 \pm 4.80$ , average decrease: 85.1%;  $P < 0.0001$ ) and day 7 (CI:  $7.87 \pm 0.26$ , CI + T:  $2.3 \pm 0.42$  average decrease: 70.8%;  $P = 0.047$ , Fig 4, I and J).

Moreover, in tubular cells, ADRA1B staining was present on the cell surface with strong nuclear pMAPK14 staining. To confirm these results, we performed sequential co-immune staining for ADRA1B and pMAPK14. As shown in the supplementary Fig 5, a majority of the tubular cells that were positive for ADRA1B had pMAPK14 staining in the nucleus of CI group compared to S group. Furthermore, there was decreased pMAPK14 in tubular cells in CI+T groups compared to CI group at D2 and D7 in both the cortex and medulla (supplementary Fig 5). There was minimal cross reactivity between the primary antibody (supplementary Fig 6, A) and the pMAPK14 and rabbit IgG<sup>26</sup> with the ADRA1B staining (supplementary Fig 6, B).

### **Terazosin treatment attenuates contrast-induced endothelin 1 (*Edn1*) and endothelin converting enzyme 1 (*Ece1*) gene expression in CKD mice kidneys.**

ADRA1B activation in endothelial cells and smooth muscle cells leads to vasoconstriction via EDN1 signaling.<sup>27,28</sup> Therefore, gene expression of *Edn1* and *Ece1* in the cortex and the medulla of the kidney were determined. There was a significant increase in the gene expression of *Edn1* in the cortex at day 2 (CI:  $3.79 \pm 0.69$ , S:  $1.1 \pm 0.21$ , average increase: 343%,  $P < 0.0001$ , Fig 5, A) with no difference at day 7. In the medulla, there was a significant increase in the average gene expression of *Edn1* at day 7 after contrast administration compared to controls (CI:  $3.41 \pm 0.79$ , S:  $1.04 \pm 0.13$ , average increase: 329.6%,  $P = 0.0002$ , Fig 5, B). Terazosin treatment (CI + T) showed a significant decrease in the average gene expression of *Edn1* in the cortex at 2 days (CI + T:  $0.23 \pm 0.12$ , CI:  $3.79 \pm 0.69$ , average decrease: 93.9%,  $P < 0.0001$ , Fig 5, A) and in the medulla at 7 days (CI + T:



$1.39 \pm 0.35$ , CI:  $3.41 \pm 0.79$ , average decrease: 59.3%,  $P = 0.0044$ , Fig 5, B) compared to contrast treated kidneys.

We next evaluated *Ece1* expression and found it was significantly increased in the cortex of CI group compared to the S group at day 2 (CI:  $2.4 \pm 0.45$ , S:  $1.1 \pm 0.19$ , average increase: 225%,  $P = 0.0002$ , Fig 5, C). At day 7 in the medulla, the average gene expression of *Ece1* was significantly higher in the kidneys from CI group compared to S group (CI:  $2.82 \pm 0.46$ , S:  $1.5 \pm 0.5$ , average increase: 228%,  $P = 0.024$ , Fig 5, D). After terazosin treatment, there was a significant decrease in the average gene expression of *Ece1* expression in the CI + T group compared to CI group in the cortex at day 2 (CI + T:  $0.28 \pm 0.09$ , CI:  $2.4 \pm 0.45$ , average decrease: 88.3%,  $P < 0.0001$ , Fig 5, C) and in the medulla at day 7 (CI + T:  $1.0 \pm 0.30$ , CI:  $2.82 \pm 0.46$ , average decrease: 64.5%,  $P = 0.0012$ , Fig 5, D).

### **Terazosin treatment attenuates contrast-induced hypoxia in the murine kidney cortex.**

We hypothesized that contrast administration causes tissue hypoxia due to vasoconstriction. We assessed for this possibility in renal tissue by performing HIF-1 $\alpha$  staining. We observed HIF-1 $\alpha$  (+) cells in both tubular cells and peritubular endothelial cells (Fig 6).

Immunohistochemical analysis demonstrated a significant increase in the cortex at 2 days after contrast administration compared to controls (CI:  $68.11 \pm 5.57$ , S:  $35.93 \pm 2.93$ , average increase: 189.56%;  $P < 0.0001$ , Fig 6, A and B) and at day 7 (CI:  $63.11 \pm 2.42$ , S:  $49.41 \pm 1.98$ , average increase: 127.73%;  $P = 0.048$ , Fig 6, A and B). In the medulla, there was a significant increase in the HIF-1 $\alpha$  staining at 2 days after contrast administration compared to controls, (CI:  $58.37 \pm 2.78$ , S:  $31.96 \pm 3.54$ , average increase: 182.63%;  $P < 0.0001$ , Fig 6, C and D) and at day 7 (CI:  $59.58 \pm 1.69$ , S:  $44.17 \pm 3.27$ , average increase: 134.89%;  $P = 0.008$ , Fig 6, C and D). Terazosin treatment significantly decreased HIF-1 $\alpha$  staining in the cortex at day 2 (CI + T:  $39.19 \pm 1.74$ , CI:  $68.11 \pm 5.57$ , average decrease: 42.46%;  $P < 0.0001$ ) and day 7 (CI + T:  $41.25 \pm 2.42$ , CI:  $63.11 \pm 2.42$  average decrease: 34.63%;  $P = 0.0006$ , Fig 6, A and B), and in medulla at day 2 (CI + T:  $32.17 \pm 2.99$ , CI:  $58.37 \pm 2.78$ , average decrease: 44.89%;  $P < 0.0001$ ) and day 7 (CI+T:  $33.22 \pm 2.06$ , CI:  $59.58 \pm 1.69$  average decrease: 44.24%;  $P < 0.0001$ , Fig 6, C and D)

### **Terazosin treatment decreases cell death and increases cell proliferation.**

ADRA1B stimulation inhibits cell proliferation and induces apoptosis via MAPK14 (p38 $\alpha$ ) activation in different cell types.<sup>26,29,30</sup> TUNEL and Ki-67 staining were performed to assess cell death and proliferation, respectively, after terazosin treatment with contrast administration. At day 2, in the cortex, kidneys removed from animals administered contrast compared to controls had a significant increase in the average TUNEL positive cells (CI:  $10.6 \pm 0.80$ , S:  $3.5 \pm 0.4$ , average increase: 302%;  $P = 0.0081$ , Fig 7, A and B) and day 7 (CI:  $13.75 \pm 3.75$ , S:  $3.66 \pm 1.04$ , average increase: 375.1%;  $P = 0.0004$ ). Terazosin treatment significantly decreased the average TUNEL positive cells compared to contrast at day 2 (CI + T:  $5.42 \pm 1.08$ , CI:  $10.59 \pm 0.80$ , average decrease: 48.9%,  $P = 0.0324$ ) and day 7 (CI + T:  $4.22 \pm 1.22$ , CI:  $13.75 \pm 3.75$ , average decrease: 69.3%,  $P = 0.0003$ ).

We next assessed TUNEL staining in the medulla. Contrast administered kidneys had a significant increase in the average TUNEL positive cells in the medulla compared to

controls at day 2 (CI:  $7.1 \pm 0.63$ , S:  $3.52 \pm 0.57$ , average increase: 201.8%;  $P = 0.0067$ , Fig 7, C and D) and day 7 (CI:  $8.95 \pm 0.99$ , S:  $4.68 \pm 1.36$ , average increase: 191.2%;  $P = 0.0016$ ). Terazosin treatment significantly decreased the average TUNEL positive cells in the medulla at day 2 (CI + T:  $4.15 \pm 0.90$ , CI:  $7.1 \pm 0.63$ , average decrease: 41.5%;  $P = 0.023$ ) and day 7 (CI + T:  $1.33 \pm 0.45$ , CI:  $8.95 \pm 1.36$ , average decrease: 85.2%;  $P < 0.0001$ ).

Next, we assessed proliferation using Ki-67 staining. There was a significant decrease in the average Ki-67 staining in contrast treated kidneys at day 2 (CI:  $5.64 \pm 1.21$ , S:  $21.29 \pm 1.57$ , average decrease: 73.5%;  $P = 0.0023$ , Fig 7, E and F) and day 7 (CI:  $7.89 \pm 0.52$ , S:  $17.25 \pm 2.57$ , average decrease: 54.3%;  $P = 0.04$ ) compared to controls. Terazosin treatment resulted in a significant increase in the average Ki-67 positive cells in the cortex of the kidney at day 2 (CI + T:  $20.28 \pm 4.1$ , CI:  $5.64 \pm 1.2$ , average increase: 359.6%,  $P = 0.0021$ ) and day 7 (CI + T:  $23.45 \pm 4.31$ , CI:  $8 \pm 0.52$ , average increase: 293.8%,  $P = 0.0017$ ).

Finally, in the medulla of kidneys removed from contrast treated animals, there was a significant decrease in the average Ki-67 staining at day 2 (CI:  $4.69 \pm 1.21$ , S:  $10.59 \pm 1.43$ , average decrease: 55.7%;  $P = 0.026$ , Fig 7, G and H) and at day 7 (CI:  $5.88 \pm 1.23$ , S:  $18.34 \pm 1.26$ , average decrease: 68%,  $P = 0.0006$ ) compared to controls. Terazosin treatment resulted in a significant increase in the average Ki-67 positive cells in the medulla of the kidney at day 2 (CI + T:  $20.72 \pm 2.52$ , CI:  $4.7 \pm 1.21$ , average increase: 442.1%;  $P < 0.0001$ ) and day 7 (CI + T:  $15.71 \pm 2.56$ , CI:  $5.88 \pm 1.23$ , average increase: 267.2%;  $P = 0.0022$ ) compared to contrast alone.

### Contrast treatment upregulates *ADRA1B* expression in HK-2 cells.

Previous studies have demonstrated that *ADRA1B* is highly expressed in tubular cells.<sup>31</sup> Therefore, *ADRA1B* expression was assessed in HK-2 cells, (epithelial cells derived from human kidney proximal tubules) after contrast treatment. The average gene expression of *ADRA1B* increased significantly over time when HK2 cells were exposed to contrast compared to controls (1h; CI:  $1.80 \pm 0.21$ , S:  $1.03 \pm 0.17$ , average increase: 175%,  $P = 0.0066$ , 12h; CI:  $2.47 \pm 0.16$ , S:  $1.005 \pm 0.072$ , average increase: 245%,  $P < 0.0001$ , Fig 8, A).

### Terazosin abrogates contrast-induced *Edn1* and *Ece1* gene expression in HK-2 cells.

We next determined the gene expression *Edn1* and *Ece1* in HK-2 cells exposed to contrast compared to S cells. There was a significant increase in the average gene expression of *Edn1* (CI:  $2.16 \pm 0.08$ , S:  $1.05 \pm 0.24$ , average increase: 205.9%,  $P = 0.0056$ , Fig 8, B) and *Ece1* (CI:  $2.1 \pm 0.23$ , S:  $1.0 \pm 0.07$ , average increase 208%,  $P = 0.0089$ , Fig 8, C) expression. Terazosin treated HK-2 cells had a significant decrease in the average gene expression of *Edn1* [CI + T:  $0.54 \pm 0.08$ , CI:  $2.16 \pm 0.08$ , average decrease: 75%,  $P = 0.0008$ , Fig 8, B) and *Ece1* [CI + T:  $0.91 \pm 0.17$ , CI:  $2.1 \pm 0.23$ , average decrease: 56.66%,  $P = 0.0058$ , Fig 8, C).

### Terazosin attenuates contrast-mediated induction of profibrotic genes in HK-2 cells.

Previous studies have demonstrated that contrast exposure upregulates profibrotic genes in HK-2 cells and in a CKD murine model.<sup>14,15</sup> We found that contrast treatment upregulated

gene expression of *Fsp-1*, a marker for the fibroblast phenotype (CI:  $3.47 \pm 0.42$ , S:  $1.01 \pm 0.11$ , average increase: 340.2%;  $P=0.0021$ , Fig 8, D), *Mmp-2* (CI:  $3.35 \pm 0.30$ , S:  $1.04 \pm 0.19$ , average increase: 323%;  $P=0.0011$ , Fig 8, E) and *Mmp-9* (CI:  $1.41 \pm 0.04$ , S:  $1.0 \pm 0.04$ , average increase: 140%;  $P=0.0021$ , Fig 8, F) compared to controls. Terazosin treatment significantly abrogated contrast-induced upregulation of *Fsp-1* (CI + T:  $1.25 \pm 0.2$ , CI:  $3.47 \pm 0.42$ , average decrease: 64.1%,  $P=0.0035$ , Fig 8, D), *Mmp-2* (CI + T:  $1.15 \pm 0.21$ , CI:  $3.35 \pm 0.30$ , average decrease: 65.7%;  $P=0.0014$ , Fig 8, E) and *Mmp-9* (CI + T:  $0.64 \pm 0.06$ , CI:  $1.41 \pm 0.04$ , average decrease: 54.3%;  $P<0.0001$ , Fig 8, F).

### Terazosin attenuates contrast-induced apoptosis in HK-2 cells.

We next sought to investigate the role of terazosin in contrast-induced apoptosis by measuring caspase 3/7 activity. As shown (Fig 8, G), contrast exposed HK 2 cells (CI) compared to control (S) group had a significant increase in the average caspase 3/7 activity (CI:  $257.4 \pm 15.08$ , S:  $100 \pm 5.26$ ; average increase: 257%,  $P<0.0001$ ). Terazosin treatment (CI + T) resulted in a significant reduction in the average caspase-3/7 activity compared to contrast (CI) alone (CI + T:  $160 \pm 9.88$ , CI:  $257.4 \pm 15.08$ , average decrease: 37.8%;  $P<0.0001$ ).

## DISCUSSION

CI-AKI can occur after intravascular administration of iodinated contrast.<sup>8,14</sup> Patients with diabetes, cardiovascular diseases and chronic kidney disease are at risk for developing CI-AKI. In order to identify the molecular mechanisms involved in CI-AKI, we performed whole transcriptome RNA-sequencing analysis with differential gene expression in kidneys after intraarterial contrast administration using a murine model with CKD.<sup>14,15</sup> This identified a set of genes related to matrix deposition, vasoconstriction,  $\alpha$ -adrenergic receptor signaling, and G-protein signaling which were upregulated in after contrast administration. Genes related to angiogenesis, anti-apoptosis, transportation, oxidoreductases and vitamin-D metabolism pathways were down regulated. We performed analysis for upstream regulator molecules to the differentially upregulated genes and this identified ADRAB1. We next validated the gene expression of ADRAB1 and then used terazosin to inhibit ADRAB1 which led to an improvement in kidney function as assessed using serum creatinine and urinary KIM-1 measurements. We also observed reduction in EDN1, ECE1 genes, with reduction in pMAPK14, hypoxic injury, and cell death with increase in proliferation. In summary, the results from this study helped identify terazosin as a potential inhibitor of CI-AKI.

In the present study, we used whole-transcriptomic analysis using RNA-sequencing which identified a set of genes related to matrix deposition, vasoconstriction,  $\alpha$ -adrenergic receptor signaling, and G-protein signaling, that were upregulated in kidneys removed from mice at 2 days after contrast administration. Genes related to angiogenesis, anti-apoptosis, transportation, oxidoreductases and vitamin-D metabolism pathways were down regulated. These data support the notion that contrast administration leads to hypoxia and an increase in apoptosis, tissue fibrosis and impaired kidney function.<sup>14,15</sup> Contrast administration leads to prolonged vasoconstriction which can cause ischemic injury leading to a reduction in

kidney function.<sup>32</sup> Diabetes and other vascular diseases can exacerbate contrast-mediated ischemic injury in patients with CKD.<sup>2,8</sup> The exact molecular mechanism or signaling cues are not known in CI-AKI. We have demonstrated that there is upregulation of *TGF- $\beta$*  signaling and tubulointerstitial fibrosis in kidneys exposed to contrast in mice with CKD.<sup>14,15</sup>

In the present study, we observed that *Adra1b*, *Col-1a1*, *Lox11*, *TGF- $\beta$ 1* and *Marcks* were up regulated in kidneys with contrast administration. Previous studies indicate that these genes are upregulated in both CKD and ESRD. These molecules are involved in matrix deposition, fibroblast activation, smooth muscle cell transduction and the EMT process.<sup>14,15,22,33,34</sup> Elevation of blood pressure and hypoxia can lead to vasoconstriction has been implicated as a potential mechanism for CI-AKI.<sup>35</sup> ADRA1B signaling plays a key role in vasoconstriction and smooth muscle cell contraction, and elevated ADRA1B levels have been reported in kidneys of ESRD patients.<sup>22,27</sup> Moreover, alpha-blockers have been used for vascular dilation.<sup>36,37</sup> *Adra1b* gene expression was significantly increased in the cortex by day 2 and in the medulla by day 2 and it remains high at day 7 after contrast administration. *In vitro* experiments further confirmed that *Adra1b* gene expression was upregulated in HK-2 cells treated with contrast media for 1 to 12 hours.

ADRA1B expression has been demonstrated to increase with ESRD progression,<sup>22</sup> vasoconstriction,<sup>27</sup> and cell transformation.<sup>38</sup> Furthermore, *EDNI* is known to decrease blood flow via vasoconstriction in the cortex.<sup>39</sup> Contrast administration significantly upregulated gene expression of *Edn1* and *Ece1* with HIF-1 $\alpha$  staining in the cortex at day 2 and in the medulla at day 7. Blockade of ADRA1B using terazosin showed a significant decrease in serum creatinine levels in the murine CKD model with contrast administration at day 2 and day 7. In addition, terazosin treatment also significantly decreased gene expression of *Edn1*, *Ece1*, along with HIF-1 $\alpha$  in mouse kidneys and in HK-2 cells. Kidney tubular cells express the endothelin system and increased endothelin signaling has also been implicated in tubular cell death in hypoxia reperfusion injury and in PC-AKI.<sup>40</sup> Terazosin treatment had also shown a significant decrease in *ADRA1B* gene expression in the kidney and in HK-2 cells which could be a due to a decrease in tissue hypoxia as a result of vasodilation. In support of this notion, chronic tissue hypoxia has shown to increase ADRA1B expression in large animals models.<sup>41</sup>

There is crosstalk between ADRA1B and MAPK14,<sup>30</sup> and MAPK14 is known to inhibit cell proliferation and induce cell death.<sup>42</sup> Moreover, it has been shown that there is upregulation of profibrotic genes, increased cell death, and decreased cell proliferation in HK-2 cells exposed to contrast agents.<sup>15</sup> This prompted us to investigate the role of ADRA1B in contrast-induced cell death. Immunohistochemical analysis indicated that there was a significant increase in pMAPK14 levels in association with increased ADRA1B in murine kidneys after contrast administration compared to kidneys from saline controls. Terazosin treatment showed a significant reduction in pMAPK14 levels along with a decrease in apoptosis and an increase in Ki-67-positive cells in kidneys exposed to contrast, with decrease in cleaved caspase-3/7 activity in HK-2 cells.

We next investigated the role of ADRA1B in contrast-induced tissue fibrosis. Interestingly, in HK-2 cells exposed to contrast, there was a significant increase in the average gene expression of *Fsp-1*, *Mmp-2* and *Mmp-9* genes. Inhibition of ADRA1B with terazosin abrogated the contrast-induced *Fsp-1*, *Mmp-2* and *Mmp-9* genes in HK2 cells. Together these results indicate ADRA1B signaling contributes to tissue fibrosis in contrast-mediated renal damage. In support of this notion, elevated *Mmp-2*, *Mmp-9* and *Fsp-1* levels have been increased in kidney damage and tissue fibrosis in hypertensive ESRD patients.<sup>43,44</sup> In summary, the results from this study demonstrate that terazosin treatment can reduce ADRA1B expression leading to improvement in kidney function after contrast administration. Future experiments need to be performed to confirm these observations.

## LIMITATIONS AND FUTURE DIRECTIONS OF THE STUDY

We acknowledge limitations of the present study, including low sample numbers (n = 3) used for *in vivo* RNA-Seq analysis. More than 95% of genes were found to be down regulated with contrast administration. Further studies are needed to address the role of down regulated genes found in the present study and to understand the role of alpha blockers in alleviating contrast-mediated toxicity and in aged mice to mimic the clinical scenario.

## Supplementary Material

Refer to Web version on PubMed Central for supplementary material.

## ACKNOWLEDGMENTS

This work was supported by National Institutes of Health grants HL098967 and DK-107870 (to S. Misra).

Data sharing: The data that support the findings of this study are available from the corresponding author on reasonable request.

## Abbreviations:

<b>Adra1b</b>	$\alpha$ -adrenergic receptor-1b
<b>CI-AKI</b>	Contrast induced acute kidney injury
<b>HK-2 cells</b>	Human kidney proximal tubule cells
<b>CKD</b>	chronic kidney disease

## REFERENCES

- Waybill MM, Waybill PN. Contrast media-induced nephrotoxicity: identification of patients at risk and algorithms for prevention. *J Vasc Interv Radiol* 2001;12:3–9. [PubMed: 11200350]
- Calvin AD, Misra S, Pflueger A. Contrast-induced acute kidney injury and diabetic nephropathy. *Nat Rev Nephrol* 2010;6: 679–88. [PubMed: 20877303]
- Wichmann JL, Katzberg RW, Litwin SE, et al. Contrast-induced nephropathy. *Circulation* 2015;132:1931–6. [PubMed: 26572669]
- Wilhelm-Leen E, Montez-Rath ME, Chertow G. Estimating the risk of radiocontrast-associated nephropathy. *J Am Soc Nephrol* 2017;28:653–9. [PubMed: 27688297]

5. Hinson JS, Ehmann MR, Fine DM, et al. Risk of acute kidney injury after intravenous contrast media administration. *Ann Emerg Med* 2017;69:577–86, e4. [PubMed: 28131489]
6. van der Molen AJ, Reimer P, Dekkers IA, et al. Post-contrast acute kidney injury - Part 1: definition, clinical features, incidence, role of contrast medium and risk factors: recommendations for updated ESUR Contrast Medium Safety Committee guidelines. *Eur Radiol* 2018;28:2845–55. [PubMed: 29426991]
7. Windpessl M, Kronbichler A. Pro: contrast-induced nephropathy-should we try to avoid contrast media in patients with chronic kidney disease? *Nephrol Dial Transplant* 2018;33:1317–9. [PubMed: 29868731]
8. McDonald JS, Leake CB, McDonald RJ, et al. Acute kidney injury after intravenous versus intra-arterial contrast material administration in a paired cohort. *Invest Radiol* 2016;51:804–9. [PubMed: 27299579]
9. Sharma A, Kilari S, Cai C, Simeon ML, Misra S. Increased fibrotic signaling in a murine model for intra-arterial contrast-induced acute kidney injury. *Am J Physiol Renal Physiol* 2020;318:F1210–F9.
10. Takahashi EA, Kallmes DF, Fleming CJ, et al. Predictors and outcomes of postcontrast acute kidney injury after endovascular renal artery intervention. *J Vasc Interv Radiol* 2017;28:1687–92. [PubMed: 28947366]
11. Palli E, Makris D, Papanikolaou J, et al. The impact of N-acetyl-cysteine and ascorbic acid in contrast-induced nephropathy in critical care patients: an open-label randomized controlled study. *Crit Care* 2017;21:269. [PubMed: 29089038]
12. Zhang JZ, Kang XJ, Gao Y, et al. Efficacy of alprostadil for preventing of contrast-induced nephropathy: a meta-analysis. *Sci Rep* 2017;7:1045. [PubMed: 28432310]
13. Quintavalle C, Brenca M, De Micco F, et al. In vivo and in vitro assessment of pathways involved in contrast media-induced renal cells apoptosis. *Cell Death Dis* 2011;2:e155. [PubMed: 21562587]
14. Sharma A, Kilari S, Cai C, Simeon ML, Misra S. Increased fibrotic signaling in a murine model for intra-arterial contrast induced acute kidney injury (CI-AKI). *Am J Physiol Renal Physiol* 2020;318(5):F1210–9.
15. Kilari S, Yang B, Sharma A, McCall DL, Misra S. Increased transforming growth factor beta (TGF- $\beta$ ) and pSMAD3 signaling in a Murine Model for Contrast Induced Kidney Injury. *Sci Rep* 2018;8:6630. [PubMed: 29700311]
16. Graham RM, Perez DM, Hwa J, Piascik MT. alpha 1-adrenergic receptor subtypes. Molecular structure, function, and signaling. *Circ Res* 1996;78:737–49. [PubMed: 8620593]
17. Hancock AA, Buckner SA, Ireland LM, Knepper SM, Kerwin JF Jr. Actions of terazosin and its enantiomers at subtypes of alpha 1- and alpha 2-adrenoceptors in vitro. *J Recept Signal Transduct Res* 1995;15:863–85. [PubMed: 8673721]
18. Taylor BN, Cassagnol M. Alpha Adrenergic Receptors. Treasure Island (FL): StatPearls; 2020.
19. Janardhanan R, Yang B, Kilari S, Leof EB, Mukhopadhyay D, Misra S. The role of repeat administration of adventitial delivery of lentivirus-shRNA-Vegf-A in arteriovenous fistula to prevent venous stenosis formation. *J Vasc Interv Radiol* 2016;27: 576–83. [PubMed: 26948326]
20. Kilari S, Cai C, Zhao C, et al. The role of microRNA-21 in venous neointimal hyperplasia: implications for targeting miR-21 for VNH treatment. *Mol Ther* 2019;27:1681–93. [PubMed: 31326400]
21. Kim D, Perteu G, Trapnell C, Pimentel H, Kelley R, Salzberg SL. TopHat2: accurate alignment of transcriptomes in the presence of insertions, deletions and gene fusions. *Genome Biol* 2013;14:R36. [PubMed: 23618408]
22. Cruz-Dominguez MP, Villalobos-Molina R, Miliar-Garcia A, et al. Evidence of alpha1-adrenoceptor functional changes in omental arteries of patients with end-stage renal disease. *Auton Autacoid Pharmacol* 2008;28:19–27. [PubMed: 18257748]
23. Dudakovic A, Camilleri E, Riester SM, et al. High-resolution molecular validation of self-renewal and spontaneous differentiation in clinical-grade adipose-tissue derived human mesenchymal stem cells. *J Cell Biochem* 2014;115:1816–28. [PubMed: 24905804]
24. Liao Y, Smyth GK, Shi W. featureCounts: an efficient general purpose program for assigning sequence reads to genomic features. *Bioinformatics* 2014;30:923–30. [PubMed: 24227677]

25. Szklarczyk D, Franceschini A, Wyder S, et al. STRING v10: protein-protein interaction networks, integrated over the tree of life. *Nucleic Acids Res* 2015;43:D447–52. [PubMed: 25352553]
26. Trempolec N, Muñoz JP, Slobodnyuk K, et al. Induction of oxidative metabolism by the p38a/MK2 pathway. *Sci Rep* 2017;7:11367. [PubMed: 28900160]
27. Adefurin A, Ghimire LV, Kohli U, et al. Genetic variation in the alpha1B-adrenergic receptor and vascular response. *Pharmacogenom J* 2017;17:366–71.
28. Lavhale MS, Briyal S, Parikh N, Gulati A. Endothelin modulates the cardiovascular effects of clonidine in the rat. *Pharmacol Res* 2010;62:489–99. [PubMed: 20826213]
29. Simão S, Fraga S, Jose PA, Soares-da-Silva P. Oxidative stress and alpha1-adrenoceptor-mediated stimulation of the Cl-/HCO3-exchanger in immortalized SHR proximal tubular epithelial cells. *Br J Pharmacol* 2008;153:1445–55. [PubMed: 18297111]
30. Waldrop BA, Mastalerz D, Piascik MT, Post GR.  $\alpha_{1B}$ - and  $\alpha_{1D}$ - adrenergic receptors exhibit different requirements for agonist and mitogen-activated protein kinase activation to regulate growth responses in rat 1 fibroblasts. *J Pharmacol Exp Ther* 2002;300:83–90. [PubMed: 11752101]
31. Uhlen M, Fagerberg L, Hallstrom BM, et al. Proteomics. tissue-based map of the human proteome. *Science* 2015;347:1260419.
32. Caiazza A, Russo L, Sabbatini M, Russo D. Hemodynamic and tubular changes induced by contrast media. *BioMed Res Int* 2014;2014:578974-.
33. Tveitaras MK, Skogstrand T, Leh S, et al. Matrix metalloproteinase-2 knockout and heterozygote mice are protected from hydronephrosis and kidney fibrosis after unilateral ureteral obstruction. *PLoS One* 2015;10:e0143390.
34. Loeffler I, Wolf G. Transforming growth factor-beta and the progression of renal disease. *Nephrol Dial Transplant* 2014;29(suppl 1):i37–45. [PubMed: 24030832]
35. Seeliger E, Sendeski M, Rihal CS, Persson PB. Contrast-induced kidney injury: mechanisms, risk factors, and prevention. *Eur Heart J* 2012;33:2007–15. [PubMed: 22267241]
36. Lipkin M, Shah O. The use of alpha-blockers for the treatment of nephrolithiasis. *Rev Urol* 2006;8(suppl 4):S35–42.
37. Saeed M, Sommer O, Holtz J, Bassenge E. Alpha-adrenoceptor blockade by phentolamine causes beta-adrenergic vasodilation by increased catecholamine release due to presynaptic alpha-blockade. *J Cardiovasc Pharmacol* 1982;4:44–52. [PubMed: 6176798]
38. Xu K, Wang X, Ling PM, Tsao SW, Wong YC. The alpha1-adrenoceptor antagonist terazosin induces prostate cancer cell death through a p53 and Rb independent pathway. *Oncol Rep* 2003;10:1555–60. [PubMed: 12883741]
39. Gurbanov K, Rubinstein I, Hoffman A, Abassi Z, Better OS, Winaver J. Differential regulation of renal regional blood flow by endothelin-1. *Am J Physiol* 1996;271:F1166–72. [PubMed: 8997390]
40. Ong AC, von Websky K, Hocher B. Endothelin and tubulointerstitial renal disease. *Semin Nephrol* 2015;35:197–207. [PubMed: 25966351]
41. Moretta D, Papamatheakis DG, Morris DP, et al. Long-term high-altitude hypoxia and alpha adrenoceptor-dependent pulmonary arterial contractions in fetal and adult sheep. *Front Physiol* 2019;10:1032. [PubMed: 31555139]
42. Desideri E, Vegliante R, Cardaci S, Nepravishta R, Paci M, Ciriolo MR. MAPK14/p38alpha-dependent modulation of glucose metabolism affects ROS levels and autophagy during starvation. *Autophagy* 2014;10:1652–65. [PubMed: 25046111]
43. Friese RS, Rao F, Khandrika S, et al. Matrix metalloproteinases: discrete elevations in essential hypertension and hypertensive end-stage renal disease. *Clin Exp Hypertens* 2009;31: 521–33. [PubMed: 19886850]
44. Nishitani Y, Iwano M, Yamaguchi Y, et al. Fibroblast-specific protein 1 is a specific prognostic marker for renal survival in patients with IgAN. *Kidney Int* 2005;68:1078–85. [PubMed: 16105038]

**AT A GLANCE COMMENTARY**

Kilari S, et al.

**Background**

Iodinated contrast is used for imaging and invasive procedures and it can cause contrast induced acute kidney injury (CI-AKI), which is the third leading hospital-acquired health problem. Currently, there are limited therapies that can reduce or prevent CI-AKI.

**Translational Significance**

The present study demonstrates that inhibition of  $\alpha$ -adrenergic receptor-1b (Adra1b) by using terazosin results in improvement in kidney function in an experimental murine model of CI-AKI.



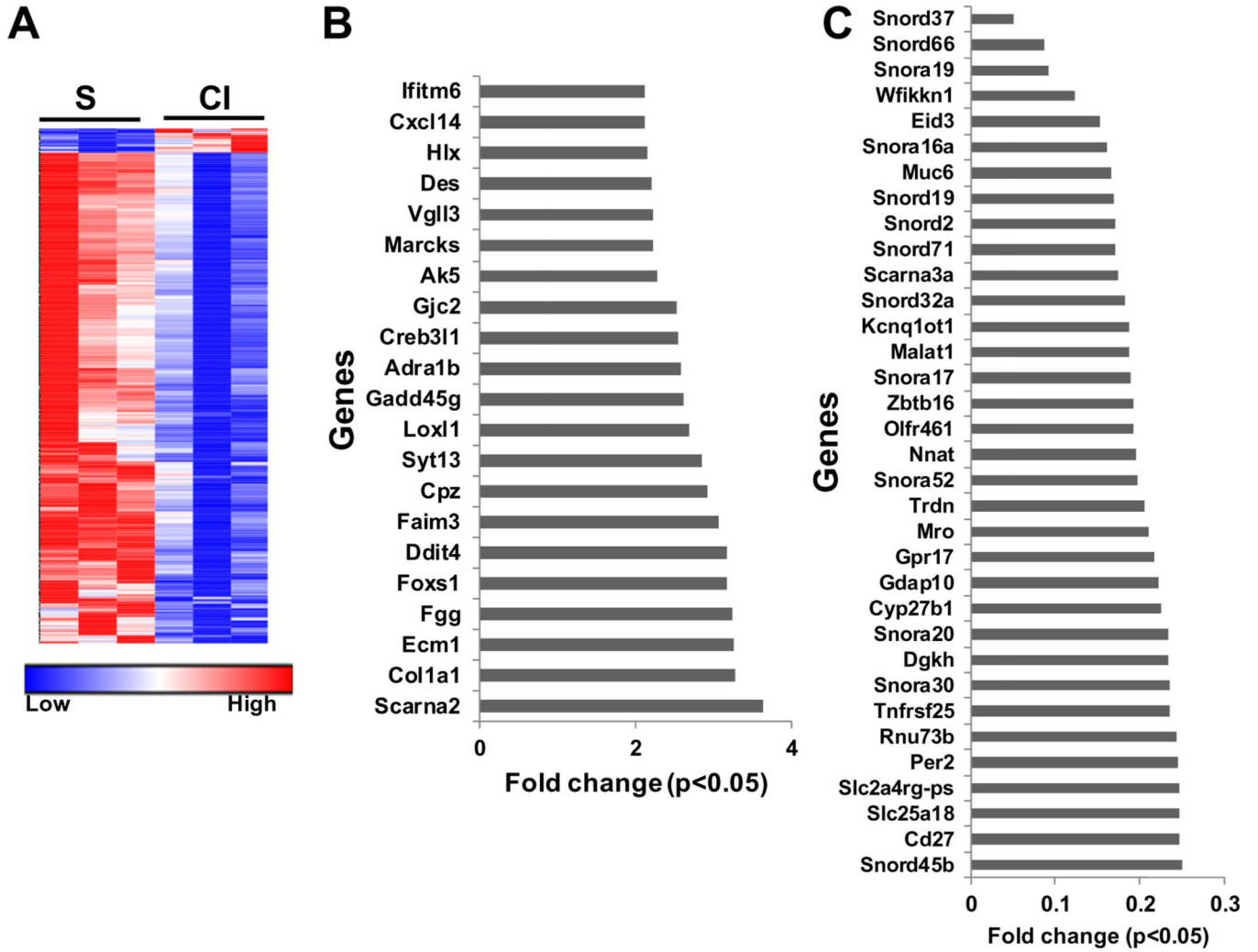


**Fig 1.** Differential gene expression profile in mice kidney at day 2 after contrast administration. Changes in mRNA expression in kidneys removed from mice two days after contrast (**CI**) or saline (**S**) administration using whole transcriptome RNA sequencing analysis. (**A**) Heat map depicting all common genes that were increased >2 fold or <0.5 fold with adjusted P <0.05 in the **CI** group compared to the **S** group. Genes that were significantly. (**B**) upregulated >2 fold and (**C**) down regulated <0.5 fold in the **CI** group compared to **S** group. Each data point represents the average (n = 3) fold change in gene expression at P < 0.05.

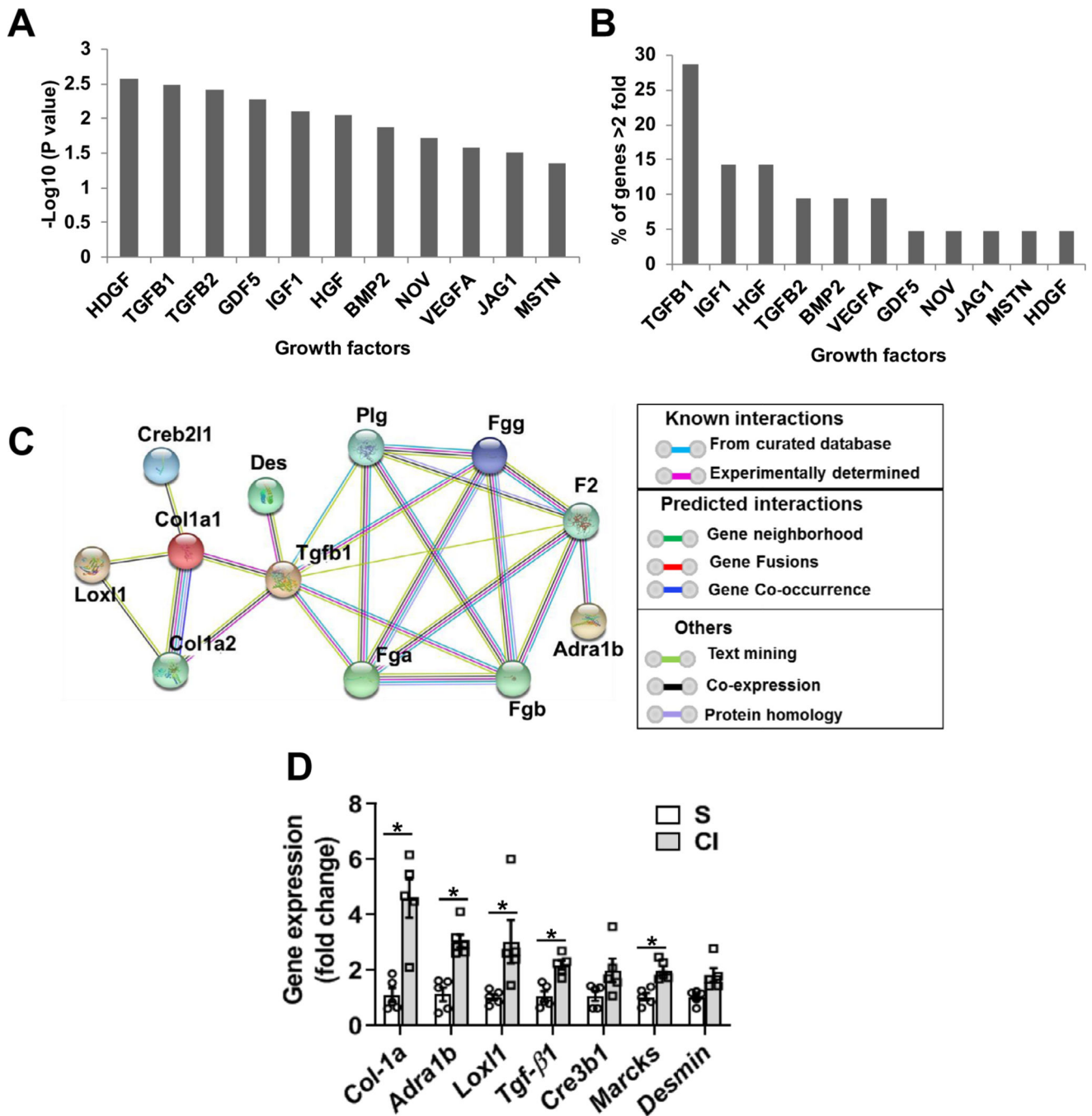


**Fig 2.** Upstream regulator analysis of genes that were >2 fold up in kidneys two days after iodine contrast administration and validation. Upstream regulator analysis was performed using the Ingenuity Pathway Analysis (IPA) tool in murine kidneys two days after contrast administration compared to saline controls. (A) Upstream regulator growth factors based on  $-\log_{10}(P\text{-value})$ , (B) Percentage of genes that were upregulated by indicated growth factor. (C) Functional protein association network analysis of genes that were regulated by TGF- $\beta$ 1 String database (<https://string-db.org/>). (D) qRT-PCR analysis of selected upregulated genes

found in the RNA-Seq data. ANOVA with repeated measurements was performed with post hoc Student *t*-test. Each bar represents mean  $\pm$  SEM of 5–7 animals per group. \* indicates  $P < 0.05$ .

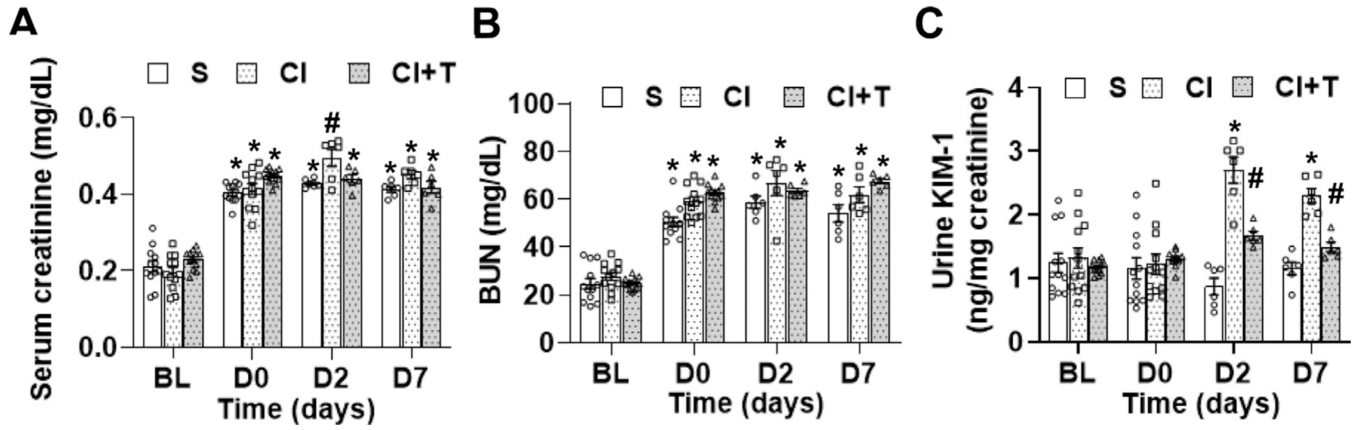


**Fig 3.** Effect of terazosin treatment on contrast-mediated elevation of serum creatinine, BUN and kidney injury molecule-1. **(A)** Serum creatinine, **(B)** blood urea and kidney injury molecule-1 were estimated at base line (BL), 28 days after nephrectomy; day 0 of contrast administration (D0), day 2 (D2) and day 7 (D7) after contrast or saline administration. Mice were administered an IP injection of 2 mg/kg terazosin in 50  $\mu$ L saline to the CI+T group or saline to the CI group and S group every 12 hours starting 1 hour before contrast administration. **S**, mice with saline administration IP; **CI**, mice with contrast administration; **CI + T**, mice with contrast administration plus terazosin IP injection. ANOVA with repeated measurements was performed with post hoc Student *t*-test. Each bar represents mean  $\pm$  SEM of 5–7 animals per group. \* indicates  $P < 0.05$ . Superscripts (\* or #) indicate a  $P < 0.05$  compared to BL data ( $P < 0.05$ ).

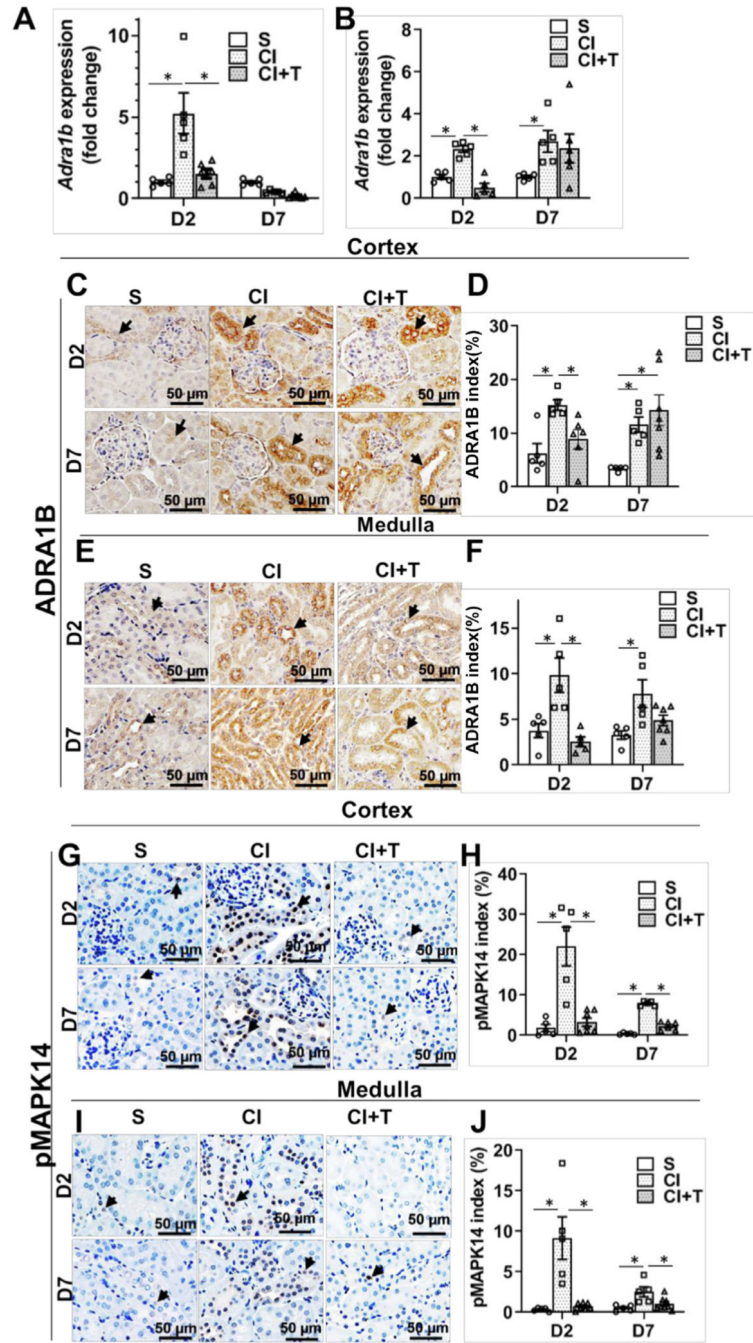


**Fig 4.** Terazosin abrogates contrast induced *Adra1B* expression and MAPK14 activation in kidney. *Adra1b* gene expression (A and B) was assessed by qRT-PCR, ADRA1B, and phospho-MAPK14 levels were determined by immunohistochemistry at day 2 or day 7 after contrast or saline administration. There was a significant increase in the *Adra1b* gene expression at day 2 and 7 after contrast administration in the cortex. Terazosin administration abrogated *Adra1b* gene expression at 2 days after contrast administration in the cortex (A) and in the medulla (B). Representative immunohistochemistry images have ADRA1B staining (C and

E) and pMAPK14 (G and I) at day 2 (D2) and day 7 (D7) after contrast administration in the cortex and in the medulla. The arrow head points to brown ADRA1B (+) staining in the tubular cells in the cortex (C) and in the medulla (E) and brown nuclear staining of pMAPK14 staining in the cortex (G) and in the medulla (I). The intensity of brown ADRA1B (+) staining in the cortex (D) and in the medulla (F) and pMAPK14 (+) in the cortex (H) and in medulla (J) was quantified using Zen Pro image analysis software. **S**, mice with saline administration+ saline IP injection; **CI**, mice with contrast administration plus saline IP injection; **CI+T**, mice with contrast administration plus terazosin IP injection. ANOVA with repeated measurements was performed with post hoc Student *t*-test. Each bar represents mean  $\pm$  SEM of 5–7 animals per group. \* indicates  $P < 0.05$ .

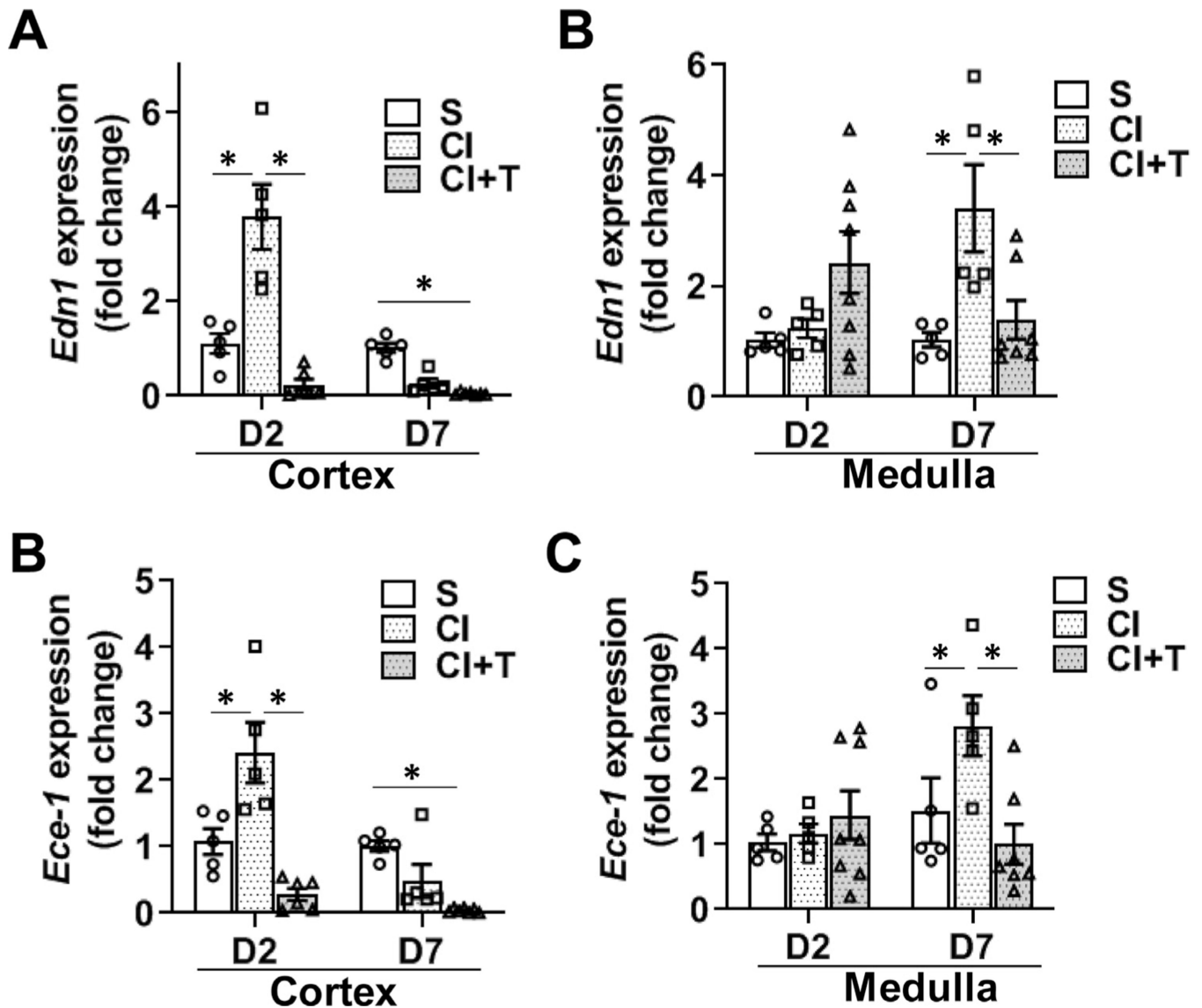
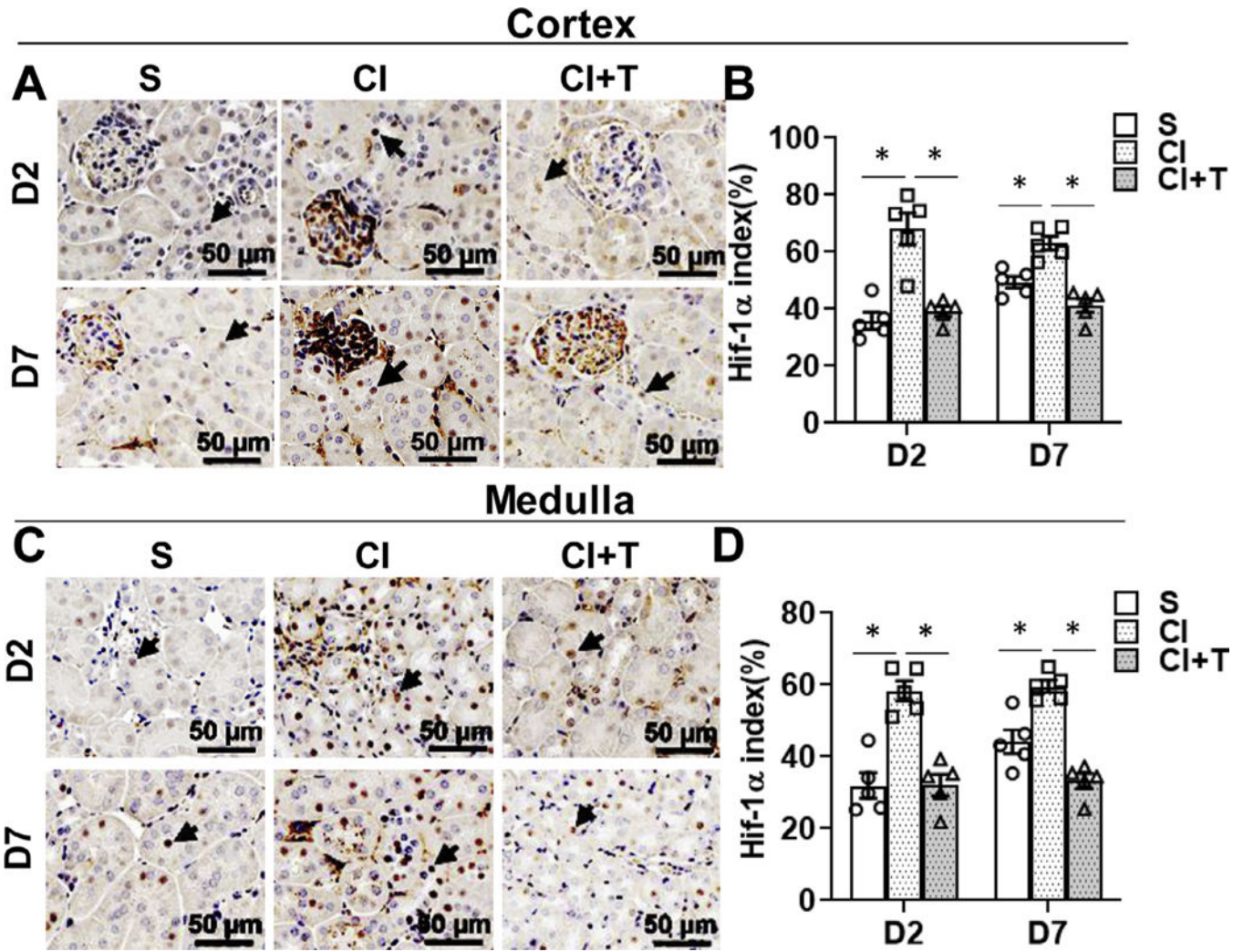


Fig 5.

Terazosin treatment abrogates contrast-induced gene expression of Endothelin-1 (*Edn1*) and Endothelin converting enzyme 1 (*Ece-1*) in kidneys. Gene expression of *Edn1* (A and B) and *Ece1* (C and D) were assessed by qRT-PCR in kidneys of mice at day 2 (D2) and day 7 (D7) after contrast administration. There is a significant increase in *Edn1* and *Ece1* expression at day 2 after CI group compared to S group kidney cortex and day 7 in kidney medulla.

Terazosin administration (CI+T) abrogated *Edn1* and *Ece1* expression in the cortex and in medulla. S, mice with saline administration IP; CI, mice with contrast administration; CI + T, mice with contrast administration plus terazosin IP injection. ANOVA with repeated measurements was performed with post hoc Student *t*-test. Each bar represents mean  $\pm$  SEM of 5–7 animals per group. \* indicates  $P < 0.05$ .



**Fig 6.** Terazosin treatment abrogates contrast-induced hypoxic response in kidneys. Hypoxia inducible factor-1 $\alpha$  (HIF-1 $\alpha$ ) was assessed by immunohistochemistry (A and C) in mouse kidneys at day 2 (D2) and day 7 (D7) after contrast (CI) or saline (S) administration. Representative Immunohistochemistry images of HIF-1 $\alpha$  protein staining in the cortex (A) and in medulla (C) at D2 and D7 of contrast administration. The arrow heads point to brown HIF-1 $\alpha$  positive nucleus in the tubular cells. The intensity of brown staining was quantified in cortex (B) and medulla (D) using Zen Pro image analysis software and presented as bar graph. S, mice with saline administration IP; CI, mice with contrast administration; CI + T, mice with contrast administration plus terazosin IP injection. ANOVA with repeated measurements was performed with post hoc Student *t*-test. Each bar represents mean  $\pm$  SEM of 5 animals per group. \* indicates  $P < 0.05$ .



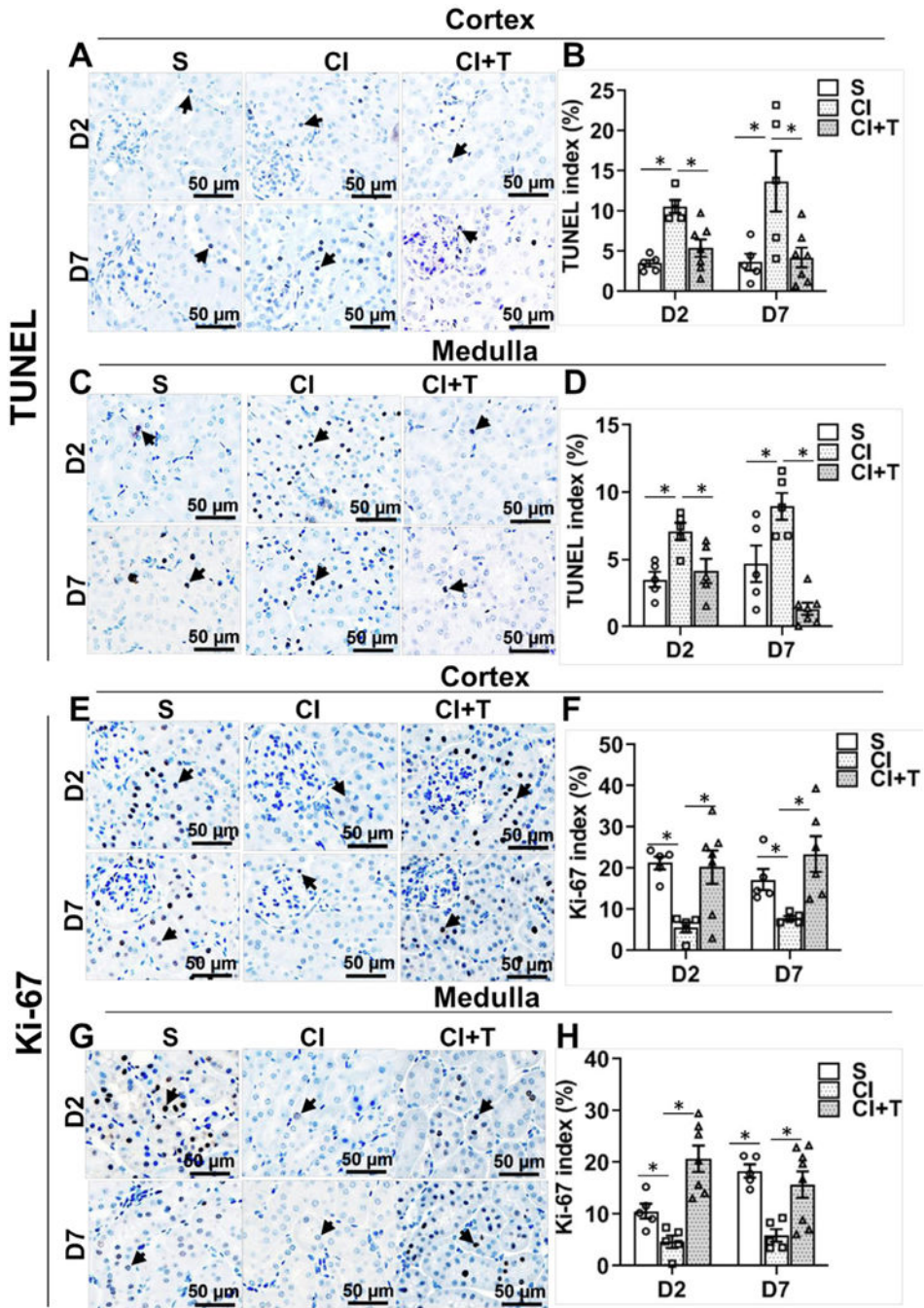


**Fig 7.** Terazosin treatment abrogates contrast-induced cell death and increases cell proliferation in kidneys. Cell death and cell proliferation were assessed by cells positive for TUNEL staining (apoptosis) and immune staining for Ki-67, respectively, in kidneys of mice at day 2 (D2) and day 7 (D7) after contrast administration. Representative images of TUNEL in cortex (A) and in medulla (C), and Ki-67 in cortex (E) and in medulla (G) staining at D2 and D7 of contrast administration. The arrow head points to brown positive nuclei for TUNEL (A and C) and Ki-67 (E and G) staining. The percentage of TUNEL or Ki-67 positive nuclei

were counted using Zen Pro image analysis software. **S**, mice with saline administration IP; **CI**, mice with contrast administration; **CI + T**, mice with contrast administration plus terazosin IP injection. ANOVA with repeated measurements was performed with post hoc Student *t*-test. Each bar represents mean  $\pm$  SEM of 5–7 animals per group. \* indicates  $P < 0.05$ .

Author Manuscript

Author Manuscript

Author Manuscript

Author Manuscript

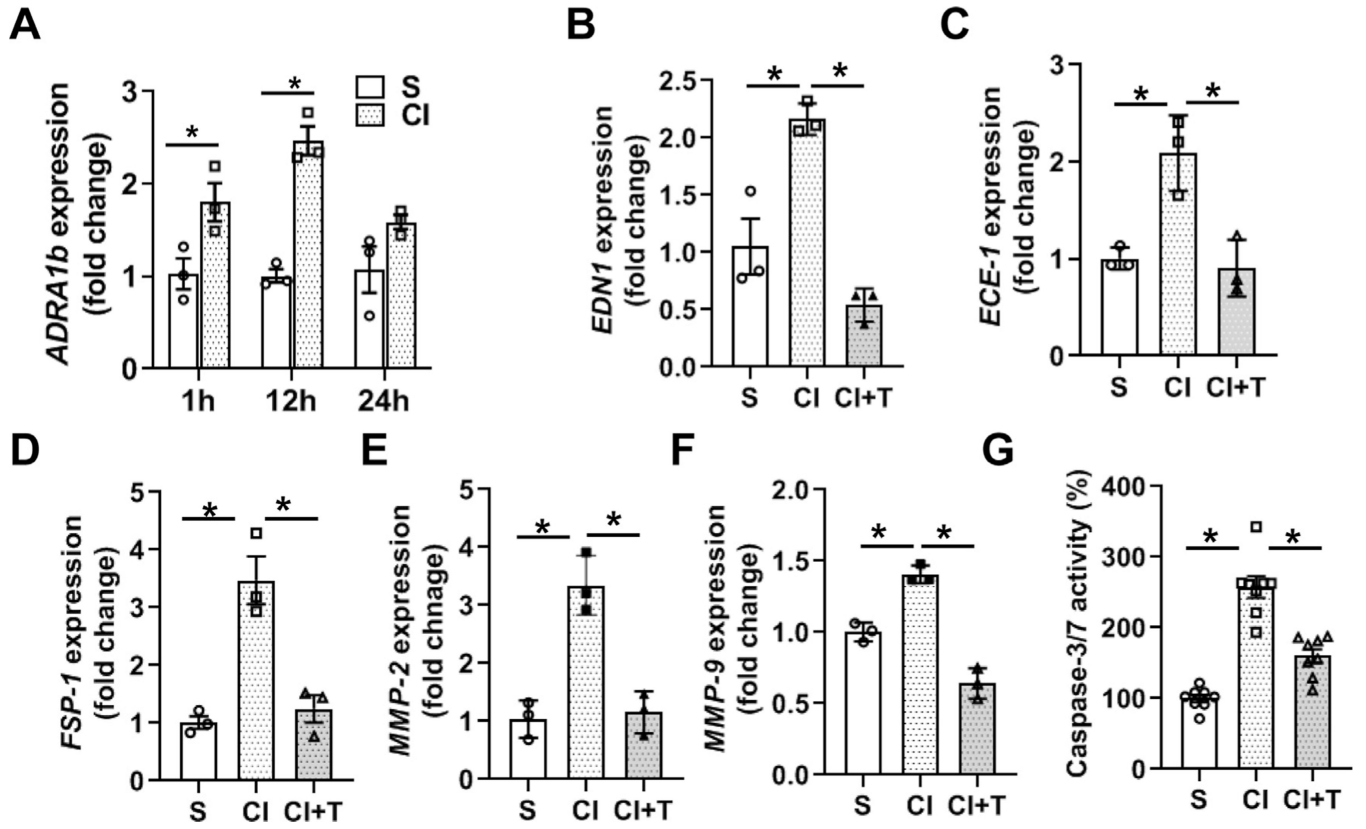


**Fig 8.**

Terazosin abrogates contrast-mediated expression of  $\alpha$ -adrenergic receptor 1b (*ADRA1B*), profibrotic genes and apoptosis in human kidney proximal tubules (HK-2). HK-2 cells were incubated with 200 mg/ml contrast media (CI) or equivalent (V/V) saline (S) in serum-free DMEM-F12 medium and gene expression was assessed by qRT-PCR. The gene expression of *Adra1B* is indicated at different time points after contrast exposure (A). Terazosin treatment abrogated contrast-induced gene expression of *Edn1* (B), *Ece1* (C), *Fsp-1* (D), *Mmp-2* (E) and *Mmp-9* (F) at 12 hours. G. Apoptosis was assessed by performing caspase 3/7 activity 24 hours after contrast exposure in the presence or absence of terazosin. ANOVA with repeated measurements was performed with post hoc Student *t*-test. Each bar represents mean  $\pm$  SEM of three independent experiments. \* indicates  $P < 0.05$ .